α-Repetition/Modulation and Blind Second-Order Identification

Philippe Ciblat, Antoine Chevreuil, and Philippe Loubaton, *Member, IEEE*

***Abstract*—In the context of redundant filter-bank precoders for blind second-order equalization, we consider the α-repetition/modulation scheme. Although it is theoretically possible, the identification of a bandlimited communication channel suffers from numerical problems *if α is beyond a bound*. If α is below this bound, simulation examples illustrate the robustness of the channel estimate.**

I. INTRODUCTION

THE TRANSMISSION of data over a dispersive unknown channel is considered. In many equalization procedures, the channel needs to be estimated. A standard solution consists in sending periodically a training sequence. However, the decrease of capacity to which this approach leads is unaffordable when the channel variations are fast. In this respect, many contributions deal with the problem of identifying the unknown channel resorting exclusively to the received signal ("blind" methods). Consistent with the fast varying environment constraint, in this paper, we focus on the second-order methods since the covariance coefficients are known to be reliably estimated by means of few samples. Thanks to [1]–[6], the fractional sampling receiver can apparently provide solutions to the blind second-order identification problem, at least when the channel exhibits an unusual condition on its zero location. All the approaches, however, fail to provide a robust estimate of the channel as far as communication channels are concerned. Indeed, the implicit cyclostationarity on which these methods rely is numerically weak due to the small excess bandwidth factors used in most communication contexts [7], [8]. For instance, such a popular algorithm as the subspace method [9] shows undesirable numerical behaviors [10].

To avoid such problems, an idea consists of increasing the strength of the cyclospectra at the receiver. This can be achieved by passing, at the emitter, the symbol sequence into a periodic precoder; the artificial cyclostationarity to which these precoders lead is referred to as transmitter induced cyclostationarity (TIC). This idea was introduced by Tsatsanis and Giannakis, who first argued in favor of a repetition of the symbols. In [12]–[14], and [26], a modulation of the symbols is shown to provide good channel estimates. In [15] and [16], a general formalism using redundant filterbanks is introduced. The blind second-order identification methods with which these precoders are associated are shown to be robust to the channel; indeed, an algebraic result states that the channel can be recovered *regardless* of the channel zero location.

The so-called α-repetition/modulation precoder (the parameter α is a real number in $[0, (1/2)]$) is a particular redundant precoder combining repetition and modulation and was introduced in [17]. As soon as α fulfills a certain nonrestrictive condition, the channel can be estimated by a structured subspace method. Contrary to the approach proposed in [14] and [26] in the context of a modulation of the symbols, the algorithm exhibits the appealing property called "deterministic." However, in the context of communication, bandlimited channel-poor performances are noticed for big α's (close to $1/2$). The contributions of the paper are 1) to explain this undesirable behavior and 2) to find the values of α for which this behavior collapses.

The α-RM transmitter is analyzed in Section II. Section III is concerned with a blind second-order based estimate of the channel by means of a noise subspace method. The extraction of the one-dimensional (1-D) kernel of a certain matrix Q_α is shown to provide the channel up to a constant. As soon as α is beyond a bound depending on the support of the channel, it is shown that Q_α exhibits a "numerical" kernel of a dimension where more than one which is spanned by spheroidal wave sequences (see Section IV). This claim is essentially based on a heuristic analysis because it is difficult to study analytically the behavior of (quasi) bandlimited FIR transfer functions. Section V is devoted to numerical illustrations.

II. DESCRIPTION OF α-RM

In the sequel, $\{s_n\}$ denotes a unit variance zero-mean i.i.d. symbol sequence with baud rate $1/T_s$. The analog impulse response of the channel is denoted by $h_a(t)$; it stems actually from the conjugate effects of a pulse shaping filter (in general, a square-root raised cosine designed for transmission at T_s) and an unknown channel due for instance to multipaths. We assume the channel to be static, in regard to the duration of observation. Without any restriction, we assume that $h_a(t)$ is causal and time limited. As the transmission is confined within a given frequency range, the frequency response of the channel is approximately bandlimited, and the frequency support is denoted by $[-((1+\gamma)/2T_s), ((1+\gamma)/2T_s)]$, where $0 \le \gamma \le 1$ is called the excess bandwidth. As far as a classical single carrier system is concerned, the received signal is simply written as

$$\sum_n s_n h_a(t - nT_s) + w_a(t) \tag{1}$$

Manuscript received May 5, 1999; revised May 30, 2000. This work was suported in part by a DGA-CNRS grant. The associate editor coordinating the review of this paper and approving it for publication was Dr. Vikram Krishnamurthy.

The authors are with the Laboratoire Systéme de Communication, University of Marne-La-Vallée, Marne-La-Vallée, France (e-mail: ciblat@univ-mlv.fr; antoine.chevreuil@univ-mlv.fr; loubaton@univ-mlv.fr).

Publisher Item Identifier S 1053-587X(00)07638-8.

1053–587X/00$10.00 © 2000 IEEE

where $\{w_a(t)\}$ is modeled as a white Gaussian noise with double-sided power density $N_0/2$. In contrast tp this standard transmission, the TIC approach proposes to transmit a transformed version of the symbol sequence—see the filterbank framework given in [15]. Precisely, the symbols are passed through a precoder. Let M and P be two integers; the output of the precoder $\{v_n\}$ is given by

$$\begin{pmatrix} v_{nP} \\ v_{nP+1} \\ \vdots \\ v_{nP+P-1} \end{pmatrix} = \begin{pmatrix} & & \\ & \mathbf{K} & \\ & & \end{pmatrix} \begin{pmatrix} s_{nM} \\ s_{nM+1} \\ \vdots \\ s_{nM+M-1} \end{pmatrix}.$$

Notice that the time between two successive v_n is $T_v = (MT_s/P)$. In order to ensure the retrieval of $\{s_n\}$ from $\{v_n\}$, it is assumed that K is a tall full-rank matrix[1] normalized in such a way that the emitted (or received) power is fixed. The received signal can be written as

$$y_a(t) = \sum_n v_n \, h_a(t - nT_v) + w_a(t). \tag{2}$$

It is worth mentioning that the required bandwidth is the same as in the single carrier case; this is due to the fact that the spectral density of $\sum_n v_n \, h_a(t - nT_v)$ is proportional to the square of the modulus of the Fourier transform of $h_a(t)$. As far as the α-RM is concerned, the precoding matrix is $2M \times M$, meaning that the baud rate of $\{v_n\}$ is twice the baud rate of $\{s_n\}$. In this paper, K is the matrix defined by blocks as

$$K = \frac{1}{\sqrt{2}} \begin{pmatrix} I_M \\ D_M(\alpha) \end{pmatrix} \tag{3}$$

with $D_M(\alpha) = \mathrm{diag}(1, e^{2i\pi\alpha}, \cdots, e^{2i\pi(M-1)\alpha})$. The received signal as given in (2) is sampled at $(1/T_v) = (2/T_s)$; we, of course, assume that prior to this sampling, $y_a(t)$ is lowpass filtered in the band $[-(1/T_s), (1/T_s)]$. Letting $y_n = y_a(n(T_s/2))$, $w_n = w_a(n(T_s/2))$, $h_k = h_a(k(T_s/2))$, and $h(z) = \sum_{k=0}^{L} h_k z^{-k}$, we get

$$y(n) = \sum_{k=0}^{L} h_k \, v_{n-k} + w_n \stackrel{\text{def}}{=} [h(z)].v_n + w_n.$$

As $\{w_n\}$ is still white, we denote by σ^2 its variance; hence, $\sigma^2 = (N_0/T_s)$. Consider the transmission of a burst of M symbols $\{s_n\}_{n=0,\, M-1}$, thus corresponding to a burst of $2M$ pseudo-symbols v_n; owing to (3), a burst is split into two consecutive bursts of length M: the first one being the burst of symbols and the second a modulated version of this latter. Up to border effects, the received data can also be split into two parts: **i**) The first one is the filtered version of the M-length burst of symbols, and **ii**) the second one is the filtered version of the modulated symbols. Consider the bivariate process $\{Y_n\}$ given by $Y_n = (y_n \; y_{n+M} \; e^{-2i\pi n\alpha})^T$. At lags $n = L, \cdots, M-1$, $\{Y_n\}$ can be expressed as

$$Y_n = \sum_{k=0}^{L} H_k^{(\alpha)} \, s_{n-k} + W_n = [H_\alpha(z)] s_n + W_n \tag{4}$$

where

$$H_\alpha(z) = \frac{1}{\sqrt{2}} \begin{pmatrix} h(z) \\ h(ze^{2i\pi\alpha}) \end{pmatrix}$$

and $W_n = (w_n \, w_{n+M} \, e^{-2i\pi n\alpha})^T$ is such that $\mathbb{E}[W_{n+\tau} W_n^*] = \sigma^2 \delta_\tau I_2$. In the sequel, the length of a burst M is supposed to be big compared with the length L of the channel: in real systems, M typically represents the number of symbols to be transmitted over a slot on which the channel can be assumed to be constant (e.g., $M = 146$ for the European GSM system). Therefore, there is no restriction in the following to just exploit vectors Y_n for $n = L, \cdots, M-1$.

The model (4) states that the α-RM artificially creates a kind of diversity. This diversity is unusual since the two components of the unknown array $H_\alpha(z)$ are deduced one from the other by a shift in the frequency domain. Intuitively, $\alpha \to 0$ makes the two components become closer, thereby making the diversity vanish; in some sense, the parameter α controls the diversity, and the choice of α is crucial. In the following sections, the blind second-order identification of $H_\alpha(z)$ and, hence, of $h(z)$, is addressed. The bivariate model (4) is similar, up to the structure, to the one encountered in classical diversity contexts; therefore, it is natural to investigate the identification problem adapting the famous noise subspace method of [9].

III. Blind Identification

A. Structured Noise Subspace Approach

Let $\hat{L}$ be an estimate of L, which is the channel order. In the sequel, it is assumed that $\hat{L} \geq L$, i.e., the model is possibly overdetermined. We propose to take into account the $M - \hat{L}$ samples $Y(n)$ for $n = \hat{L}, \cdots, M-1$ in order to estimate the channel. Take $N < M - \hat{L}$. We consider the big vector $\mathcal{Y}_n = (Y_n^T, Y_{n-1}^T, \cdots, Y_{n-N}^T)^T$ for the lags $n = N + \hat{L}, \cdots, M-1$. It is readily seen that

$$\mathcal{Y}_n = \underbrace{\begin{pmatrix} H_0^{(\alpha)} & H_1^{(\alpha)} & \cdots & H_L^{(\alpha)} & 0 & \cdots & 0 \\ 0 & H_0^{(\alpha)} & H_1^{(\alpha)} & \cdots & H_L^{(\alpha)} & \ddots & \vdots \\ \vdots & & & & & & 0 \\ 0 & \cdots & 0 & H_0^{(\alpha)} & H_1^{(\alpha)} & \cdots & H_L^{(\alpha)} \end{pmatrix}}_{\mathcal{T}(H_\alpha)} \cdot \mathcal{S}_n + \mathcal{W}_n$$

where $\mathcal{S}_n = (s_n, s_{n-1} \cdots, s_{n-N-L})^T$, and $\mathcal{W}_n = (W_n^T, W_{n-1}^T, \cdots, W_{n-N}^T)^T$. $\mathcal{T}(H_\alpha)$ is the $2(N+1) \times (L+N+1)$ Sylvester matrix associated with the filter $H_\alpha(z)$. The $(N+1)$-dimensional covariance matrix of $\{Y_n\}$ is simply $\mathcal{R} = \mathcal{T}(H_\alpha)\mathcal{T}(H_\alpha)^* + \sigma^2 I_{2(N+1)}$.

[1]which imposes that $P \geq M$ or equivalently that $T_v \leq T_s$.

We choose N such that the matrix $\mathcal{T}(H_\alpha)$ is tall, namely, one chooses $\hat{L}+1 \leq N < M-\hat{L}$. This implies that $\mathcal{T}(H_\alpha)\mathcal{T}(H_\alpha)^* = \mathcal{R}-\sigma^2 I_{2(N+1)}$ is a singular matrix. Denote by Π the orthogonal projector onto its kernel. Take $f(z)=\sum_{k=0}^{\hat{L}} f_k z^{-k}$ to be a generic $\hat{L}$-order polynomial, and denote by $F_\alpha(z) = (1/\sqrt{2})(f(z),\, f(ze^{2i\pi\alpha}))^T$ its associated bivariate structured polynomial. The subspace method consists in investigating the mapping

$$f \mapsto \mathrm{Trace}(\Pi \mathcal{T}(F_\alpha)\mathcal{T}(F_\alpha)^*\Pi^*).$$

This is a quadratic form in the coefficients (f_k). Letting $\boldsymbol{f} = (f_0, f_1, \cdots, f_{\hat{L}})^T$, the subspace mapping can be written as $\boldsymbol{f}^* Q_\alpha \boldsymbol{f}$ for a certain $(\hat{L}+1)$-dimensional positive Hermitian matrix Q_α. We decompose Π as $\Pi = [\Pi_0, \cdots, \Pi_N]$, where each matrix Π_k is $2(N+1)\times 2$. If $\Pi(e^{2i\pi f}) = \sum_{k=0}^{N} \Pi_k e^{-2i\pi k f}$, the matrix Q_α is expressed as

$$Q_\alpha = \mathcal{P}^* D_\Pi^* D_\Pi \mathcal{P} \tag{5}$$

where

$$D_\Pi = \int_{-1/2}^{1/2} \overline{D_{N+\hat{L}}(e^{2i\pi f})}\, D_{\hat{L}}^T(e^{2i\pi f}) \otimes \Pi(e^{2i\pi f})\, df \tag{6}$$

and $\mathcal{P}$ is a block-diagonal structure matrix, which is the kth 2×1 block given by $(\mathcal{P})_k = [1,\, e^{-2i\pi k\alpha}]^T$. For any integer k, the directional vector of order k is defined as $D_k(e^{2i\pi f}) = (1,\, e^{-2i\pi f}, \cdots, e^{-2i\pi k f})^T$. The theorem below gives a condition on α for the channel to be retrieved up to constant from Q_α. We now have the following theorem.

Theorem 1 (Identifiability): Suppose α is rational, namely, $\alpha = (p/q)$ with p and q coprime. If $q \geq \hat{L}$, the kernel of the matrix Q_α is a 1-D subspace spanned by the channel vector

$$\boldsymbol{h} = (h_0, h_1, \cdots, h_L, \underbrace{0, \cdots, 0}_{\hat{L}-L})^T.$$

In others words, the structured noise subspace method allows identification of the filter $h(z)$ up to a scalar.

This algebraic result is proved in [12]–[14], and [26] and devoted to the modulation TIC precoder. Notice that in contrast with the classical nonstructured subspace method, the unknown filter is recovered irrespective of the channel zero location and whatever the overdetermination factor.

Remark: For sake of clarity, we suppose in the sequel that $\hat{L} = L$. Moreover, it is implicitly assumed that α fulfills the condition of Theorem 1.

B. Estimate of the Channel

In practice, a finite number of data is collected, and the matrix $\mathcal{R}$ is estimated from these data. We denote by $T = M - L$ the number of available samples Y_n; for simplification, we reindex the data and denote them by $\{Y_n\}_{n=0,\,T-1}$. From these data, one has to estimate the Toeplitz matrix $\mathcal{R}$ and then the projector Π. Consider the matrix

$$\hat{\mathcal{R}} = \frac{1}{T}\sum_{n=0}^{T-1} \mathcal{Y}_n \mathcal{Y}_n^*.$$

We estimate the projector Π by $\hat{\Pi}$, which is the orthogonal projector onto the space generated by the eigenvectors associated with the smallest eigenvalues of $\hat{\mathcal{R}}$. The quadratic matrix Q_α is estimated by

$$\hat{Q_\alpha} = \mathcal{P}^* D_{\hat{\Pi}}^* D_{\hat{\Pi}} \mathcal{P}$$

and the channel $\boldsymbol{h}$ by[2]

$$\hat{\boldsymbol{h}}_T = \arg\min_{\|f\|=1} \boldsymbol{f}^* \hat{Q}_\alpha \boldsymbol{f}.$$

Notice that in the noise-free case, the estimate $\hat{\mathcal{R}}$ is simply

$$\hat{\mathcal{R}} = \mathcal{T}(H_\alpha)\left(\frac{1}{T}\sum_{n=0}^{T-1} \mathcal{S}_n \mathcal{S}_n^*\right)\mathcal{T}(H_\alpha)^*$$

and the extraction of the projector Π can be done exactly with a finite number of samples. Hence, $\hat{\boldsymbol{h}}_T$ and $\boldsymbol{h}$ coincide up to a constant; the algorithm is called deterministic. This is in contrast with the structured subspace algorithm used in [14] and [26] in the context of modulation TIC precoders.

C. Statistical Performances

It is standard (see [18]) that $\sqrt{T}(\hat{\boldsymbol{h}}_T - \boldsymbol{h})$ converges weakly to a zero mean normal random vector with covariance matrix

$$C = Q_\alpha^{\#} \mathcal{P}^* D_\Pi^* \Sigma D_\Pi \mathcal{P} Q_\alpha^{\#} \tag{7}$$

where $(.)^{\#}$ stands for the pseudoinverse, and Σ is a certain nonnegative matrix.

D. Existence of an Undesired Numerical Kernel

In the context of communication channels, it has been noticed that for certain choices of α, Q_α exhibits a 1-D kernel, as expected from Theorem 1, but also has eigenvectors associated with "small" eigenvalues. Of course, such a phenonenon prevents the subspace algorithm from showing good performances; indeed, because the exact kernel of Q_α and its numerical kernel are difficult to separate, the estimate $\hat{\boldsymbol{h}}_T$ is likely to belong to a corrupted version of the numerical kernel of Q_α. Moreover, from (7), the existence of these small eigenvalues makes the covariance matrix huge in the direction of the associated eigenvectors. This phenonenon is now specified.

IV. Existence and Analysis of the Numerical Kernel of Q_α

A. A Qualitative Remark

In the following, we denote by $(1/2) \leq \beta \leq 1$ the bandwidth of the channel sampled at $2/T_s$. This quantity is related to the excess bandwidth parameter since $\beta = ((1+\gamma)/2)$ (see Fig. 1). We assume, for sake of clarity, a noiseless case. Denote by $S(e^{i2\pi f})$ the spectrum of the bivariate process $\{Y_n\}$. As $\{s_n\}$ is white, we have

$$S(e^{i2\pi f}) = H_\alpha(e^{i2\pi f}) H_\alpha(e^{i2\pi f})^*. \tag{8}$$

[2]This is not a proper definition since this the phase indetermination remains. This problem is out of the scope of the paper, as we aim to identify the channel up to a constant.

The statistical information is contained in the components $(1, 1)$ and $(1, 2)$ of $S(e^{i2\pi f})$, i.e., in $|h(e^{i2\pi f})|^2$ and $h(e^{i2\pi f})h(e^{i2\pi(f+\alpha)})^*$; as $h(e^{i2\pi f})$ is bandlimited, the term $h(e^{i2\pi f})h(e^{i2\pi(f+\alpha)})^*$ is all the less relevant as α is close to $1/2$ ("big" α's); in this case, the (numerical) supports of $h(e^{i2\pi f})$ and $h(e^{i2\pi(f+\alpha)})^*$ have a narrow intersection, making their product small. For instance, if the excess bandwidth is zero (in this case, $\gamma = 0$ and $\beta = 1/2$), the quantity $h(e^{i2\pi f})h(e^{i2\pi(f+\alpha)})^*$ is null for $\alpha = 1/2$. The spectral density $S(e^{i2\pi f})$ thus provides only $|h(e^{i2\pi f})|^2$, which is, of course, not sufficient to identify $h(e^{i2\pi f})$. The closer α is to $1/2$, the more numerical problems are expected. That α should be upper bounded is now specified.

B. Short Review on Spheroidal Wave Sequences

The order $L+1$ spheroidal wave sequences ([19]) on an interval $\mathcal{I}$ are the (unit norm) eigenvectors $\{\boldsymbol{k}_j\}_{j=0, L}$ associated with the eigenvalues $\lambda_0 \leq \cdots \leq \lambda_L$ of the positive $(L+1) \times (L+1)$ Toeplitz matrix $\mathcal{K}_{\mathcal{I}, L}$, which is defined as

$$\mathcal{K}_{\mathcal{I}, L} = \int_{\mathcal{I}} \overline{D_L(e^{2i\pi f})} D_L^T(e^{2i\pi f})\, df.$$

They play an important role in various problems involving implicitly bandlimited signals, for instance, in bandlimited spectral estimation [20]), broadband source localization [21], array beam-forming ([22]), etc. The matrix $\mathcal{K}_{\mathcal{I}, L}$ is known to be ill conditioned, and its "numerical" rank is equal to int$((L+1)|\mathcal{I}|)$, where int(.) stands for the integer part of (.) and where $|\mathcal{I}|$ represents the size of $\mathcal{I}$. In the following, we denote by s the dimension of the numerical kernel of $\mathcal{K}_{\mathcal{I}, L}$. For a given $\boldsymbol{k}_j = (k_{j,0}, \cdots, k_{j,L})$, we let the associated transfer function be $k_j(z) = \sum_{l=0}^{L} k_{j,l} z^{-l}$. As $\boldsymbol{k}_j^* \mathcal{K}_{\mathcal{I}, L} \boldsymbol{k}_j$ is given by

$$\boldsymbol{k}_j^* \mathcal{K}_{\mathcal{I}, L} \boldsymbol{k}_j = \int_{\mathcal{I}} \left| k_j(e^{2i\pi f}) \right|^2 df$$

the existence of a numerical kernel of $\mathcal{K}_{\mathcal{I}, L}$ implies that for $j < s$

$$k_j(e^{2i\pi f}) \approx 0 \quad \text{if} \quad f \in \mathcal{I}.$$

In others words, the FIR filters $k_j(e^{i2\pi f})$ for $j = 0, s-1$ associated with the s so-called "smallest" spheroidal wave sequences of $\mathcal{I}$ are nearly bandlimited, and their support coincides with the complementary set of $\mathcal{I}$ in $[-(1/2), (1/2)]$.

C. Numerical Kernel of Q_α

In this section, we justify, by means of heuristic arguments, that Q_α may exhibit, in addition to its natural 1-D kernel, a undesired numerical kernel. This is proved to occur when α is too big. We claim the following.

Claim 1: If $\alpha > (\beta/2)$, Q_α exhibits a numerical kernel of dimension more than 1; actually

$$\dim \text{Ker}(Q_\alpha) \gtrsim 1 + \text{int}((L+1)(2\alpha - \beta)).$$

In this case, denote by $\mathcal{W}$ the interval

$$\mathcal{W} = \left[\frac{\beta}{2} - \alpha, \quad \alpha - \frac{\beta}{2} \right].$$

The linear space spanned by the true channel $\boldsymbol{h}$ and the smallest spheroidal wave sequences of length $L+1$ of the interval[3] $\mathcal{W}^c$ belong to the numerical kernel of Q_α. As a consequence, the asymptotic covariance of the subspace estimate is huge in the band $\mathcal{W}$.

A justification is proposed in the Appendix.

D. Consequence

Within this section, it is assumed that $\alpha > \beta/2$. Let s be $s = \text{int}((L+1)(2\alpha - \beta))$. Consider a vector $\boldsymbol{l}$ of the numerical kernel of Q_α—recall that the channel estimate is likely to be close to such a vector. According to Claim 1, $\boldsymbol{l}$ may be a linear combination of $\boldsymbol{h}$ and some of the s smallest spheroidal wave sequences of the band $\mathcal{W}^c$, which are denoted by $(\boldsymbol{k}_j)_{j=0, s-1}$; in the frequency domain, this implies that

$$l(e^{i2\pi f}) = \sum_{j=0}^{s-1} r_j k_j(e^{i2\pi f}) + r_s h(e^{i2\pi f})$$

for some complex-valued constants (r_j). However, $k_j(e^{i2\pi f}) \approx 0$ when $f \in \mathcal{W}^c$, but this is not the case if $f \in \mathcal{W}$. In other words, the subspace cannot provide a reliable estimate of the channel (up to a constant) in the band $\mathcal{W}$. The second part of Claim 1 gives an insightful consequence of the existence of a numerical kernel on a statistical point of view. Indeed, due the terms $Q_\alpha^\#$ in (7), the asymptotic covariance matrix C is prone to exploding in the directions of the spheroidal wave sequences $(\boldsymbol{k}_j)_{j=0, s-1}$. Consider the quantity

$$\left| E(e^{i2\pi f}) \right|^2 = T\, \mathbb{E} \left| \hat{h}_T(e^{i2\pi f}) - h(e^{i2\pi f}) \right|^2$$

which represents the localization in the frequency domain of the mean square error. We have, for large T, $|E(e^{i2\pi f})|^2 \approx$ trace$(C\overline{D_L(e^{i2\pi f})}D_L^T(e^{i2\pi f}))$. We consider the average of the mean square error on the interval $\mathcal{W}$. It can be shown to verify

$$\int_{\mathcal{W}} \left| E(e^{i2\pi f}) \right|^2 df = \text{trace}(C\mathcal{K}_{\mathcal{W}, L}).$$

As C may be explosive in the directions of the sequences $(\boldsymbol{k}_j)_{j=0, s-1}$, the mean square error is thus likely to be huge in the band $\mathcal{W}$; the estimate is not reliable in this band of frequencies.

Remark 2: Conversely, the condition $\alpha \leq (\beta/2)$ does not ensure that the numerical kernel is reduced to the span of $\boldsymbol{h}$; however, the previous bandwidth considerations cannot prove the contrary. The simulation evidence (see Section V) illustrates that the condition $\alpha \leq (\beta/2)$ is sufficient to ensure that the numerical kernel is 1-D in a typical transmission context. Of course, α should not be taken too close from 0 in order to ensure a good diversity between the two components of Y_n.

E. Fractional Sampling (FS) and α-RM

The FS receiver consists in sampling the signal given by (1) at the baud-rate $2/T_s$. The discrete (noiseless) time series is

$$y_n^{(fs)} = [h(z)].\tilde{s}_n$$

[3] $\mathcal{W}^c$ denotes the complementary set of $\mathcal{W}$ in $[-(1/2), (1/2)]$.

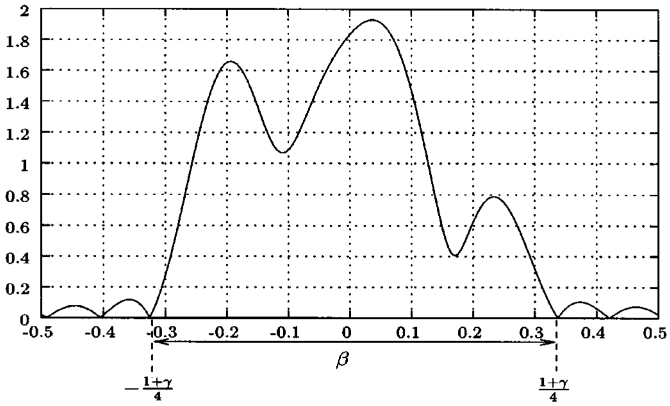

Fig. 1. Power transfer function $|h(e^{i2\pi f})|^2$.

where $h(z)$ and w_n are the same as in α-RM. This time, $\{\tilde{s}_n\}$ is the series obtained by inserting a zero between two consecutive symbols. The process $y_n^{(fs)}$ is periodically correlated since the autocorrelation function $R(n,\tau) = \mathbb{E}y_{n+\tau}^{(fs)}y_n^{(fs)*}$ is periodic of period 2 in the variable n. The cyclocorrelation coefficients of $y_n^{(fs)}$ are defined as $R^{(0)}(\tau) = (1/2)(R(0,\tau) + R(1,\tau))$ and $R^{(1)}(\tau) = (1/2)(R(0,\tau) - R(1,\tau))$. The jth cyclospectrum $S^{(j)}(e^{i2\pi f})$ is the discrete Fourier transform of $(R^{(j)}(\tau))_\tau$. Gather the second-order statistics into the spectral matrix

$$\mathcal{S}(e^{i2\pi f}) = \begin{pmatrix} S^{(0)}(e^{i2\pi f}) & S^{(1)}(e^{i2\pi f}) \\ S^{(1)}(e^{i2\pi f})^* & S^{(0)}(e^{i2\pi f}) \end{pmatrix}.$$

It is straightforward that $\mathcal{S}(e^{i2\pi f})$ is expressed as

$$\mathcal{S}(e^{i2\pi f}) = H_{1/2}(e^{i2\pi f})H_{1/2}(e^{i2\pi f})^*.$$

A subspace method lying on this set of statistics can be used to extract the channel [23], [24] if and only if $H_{1/2}(z)$ is nonzero[4] for all z (including ∞). In this case, the orthogonal projector is precisely the one encountered in α-RM for $\alpha = 1/2$, hence making the quadratic subspace matrix coincide with $Q_{1/2}$. Hence, the analysis of Section IV holds for this spectral factorization method: The estimate is not reliable in the band of frequencies $[-((1-\beta)/2), ((1-\beta)/2)]$. As far as the standard approach of [9] is concerned, denote the quadratic matrix by Q_{fs}; unfortunatly, the link between $Q_{1/2}$ and Q_{fs} is not easily seen. However, as is shown in [10] and [25], the smallest spheroidal sequences of $[-((1-\beta)/2), ((1-\beta)/2)]^c$ also belong to the numerical kernel of Q_{fs}, thereby creating a link between 1/2-RM and FS.

V. Numerical Illustrations

We consider the matrix Q_{fs} of [9], which was evoked in Section IV-E, as a point of comparison.

A. *On the Existence of a Numerical Kernel and its Structure*

Consider the communication channel the power transfer function of which is represented in Fig. 1; this channel corresponds to an excess bandwidth factor $\gamma = 0.2$ (i.e., $\beta = 0.6$) and to a multipath realization given in Table I. The complete impulse response is truncated such that 1% of the total energy is removed. This makes $h(z)$ be a degree $L = 11$ polynomial.

[4]This condition is equivalent to the condition that the two polyphase components of $h(z)$ have no common zeros.

TABLE I
Multipath Realization

Attenuations	-0.65+1.52i	2.81-0.08i	-0.42+0.47i	-0.59-0.47i	-1.33+1.31i	2.03 + 0.56i
Delays ($\times T_s$)	0	0.16	1.13	1.81	2.04	2.48

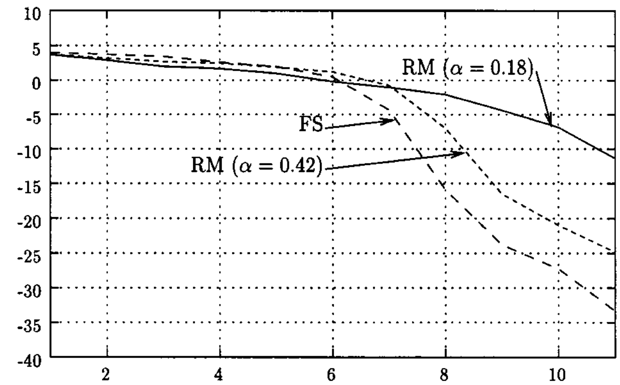

Fig. 2. Non-null eigenvalues of $(Q_\alpha)_{\alpha=0.18,\,0.42}$ and Q_{fs} in decibels.

TABLE II
Spheroidal Effect

	FS	RM ($\alpha = 0.42$)
Dimension of the extra numerical kernel	4	2
$\{\mathbf{k}_j^* Q \mathbf{k}_j,\ j = 0, \ldots, s-1\}$	0.0018 0.0028 0.0080 0.0619	0.004 0.025

All the nonnull eigenvalues of Q_α for $\alpha \in (0.18, 0.42)$ and of Q_{fs} are represented in Fig. 2. Notice that for $\alpha = 0.42$ and for the FS case, the existence of a numerical kernel is clearly exhibited; this is coherent with the analysis led in Section IV, in which the existence of a numerical kernel is proved to occur as soon as $\alpha > \beta/2$, i.e., $\alpha > 0.3$. More precisely, the dimension of the numerical kernel of Q_α, for $\alpha = 0.42$, is given in Table II. Furthermore, the values $\boldsymbol{k}_j^*(Q_\alpha)_{\alpha=0.42}\boldsymbol{k}_j$ are computed for all the smallest spheroidal wave sequences $\boldsymbol{k}_j$ relative to the "corrupted" band $[-0.12, 0.12]$. The same quantities are computed for Q_{fs}, for which this interval is $[-0.2, 0.2]$. The results corroborate our analysis since the $(\boldsymbol{k}_j)_{j=0,\,s-1}$ belong clearly to the numerical kernel (indeed, $\boldsymbol{k}_j^* Q_\alpha \boldsymbol{k}_j$ and $\boldsymbol{k}_j^* Q_{fs} \boldsymbol{k}_j$ are small).

Consider the case of $\alpha = 0.42$. The excess bandwidth varies from 20% to 100%. The analysis in Section IV shows that spheroidal effects are expected to occur as soon as $(\beta/2) \le \alpha$. As $\beta = ((1+\gamma)/2)$, this gives $\gamma \le 0.68$. In Fig. 3, the smallest non-null eigenvalue of Q_α is represented as a function of γ. Remarkably, the case $\gamma \gtrapprox 0.68$ corresponds to a good conditioning of Q_α, whereas this conditioning is all the worse as γ decreases, as expected by our heuristic analysis.

B. *Impact of the Numerical Kernel on the Statistical Performance*

Within this section, the SNR is 30 dB.

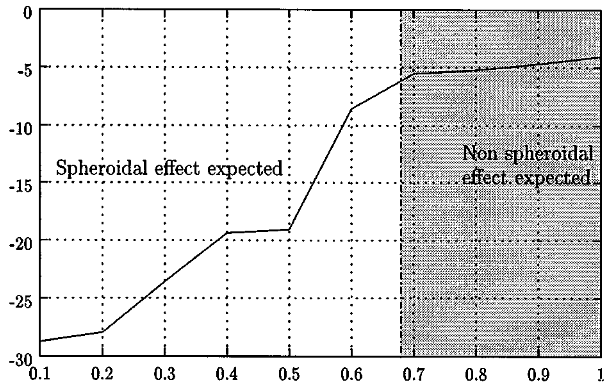

Fig. 3. Smallest non-null eigenvalue (in decibels) of $(Q_\alpha)_{\alpha=0.42}$ versus roll off.

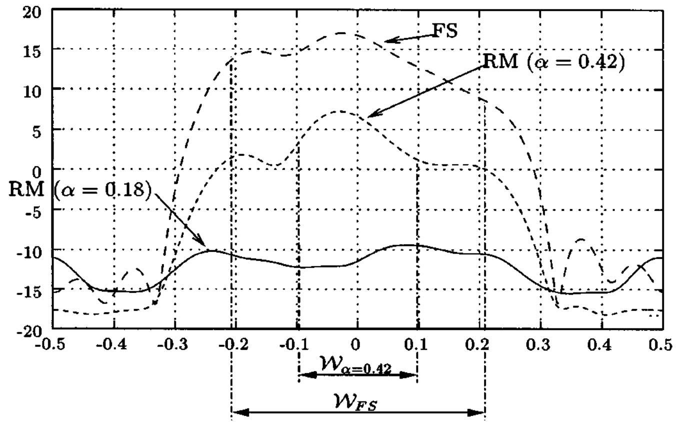

Fig. 4. $T\,\mathbb{E}|\hat{h}_T(e^{2i\pi f}) - h(e^{2i\pi f})|^2$ in decibels for "large" T.

Channel 1 is considered (recall that $\gamma = 0.2$). In the frequency domain, let us now represent $T\,\mathbb{E}|\hat{h}_T(e^{i2\pi f}) - h(e^{i2\pi f})|^2$ for large T; we considered the FS and the α-RM for $\alpha \in (0.18,\ 0.42)$ cases. The analysis given in Sections IV and III-C shows that $T\,\mathbb{E}|\hat{h}_T(e^{i2\pi f}) - h(e^{i2\pi f})|^2$ is expected to be huge in the band of frequencies $\mathcal{W}$ when this interval is not empty, i.e., for the FS and $\alpha = 0.42$. In Fig. 4, the functions $T\,\mathbb{E}|\hat{h}_T(e^{i2\pi f}) - h(e^{i2\pi f})|^2$ are plotted in the cases above specified.

- *FS case*: $\mathcal{W} = [-0.2,\ 0.2]$; indeed, the covariance is huge within this range.
- $\alpha = 0.42$: $\mathcal{W} = [-0.12,\ 0.12]$; the covariance is big within this band of frequencies.
- $\alpha = 0.18$: $\mathcal{W} = \emptyset$. The covariance is approximatly constant. The estimate is reliable.

Last, we consider once again the excess bandwidth as a variable. It is proposed to evaluate trace(C), which represents T times the mean square error $\mathbb{E}\sum_{k=0}^{L}|\hat{h}_{T,k} - h_k|^2$ for different values of γ. The results are put in Fig. 5. This shows that the case $\alpha = 0.18$ is not sensitive to a variation of γ, whereas in the case where $\alpha = 0.42$, one should have γ more than a threshold in order to ensure a good behavior (the analysis gives $\gamma \gtrsim 0.68$, and in fact, one should not choose $\gamma < 0.4$). As far as the FS system is concerned, one should choose $\gamma \approx 1$ to ensure a good performance; indeed, the interval $\mathcal{W}$ is never empty, whatever $0 < \gamma < 1$.

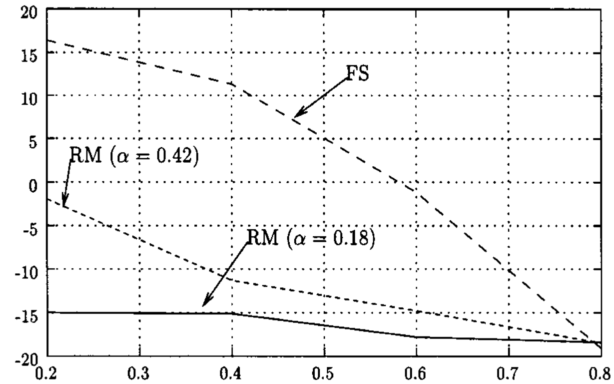

Fig. 5. Trace(C) (in decibels) versus roll off.

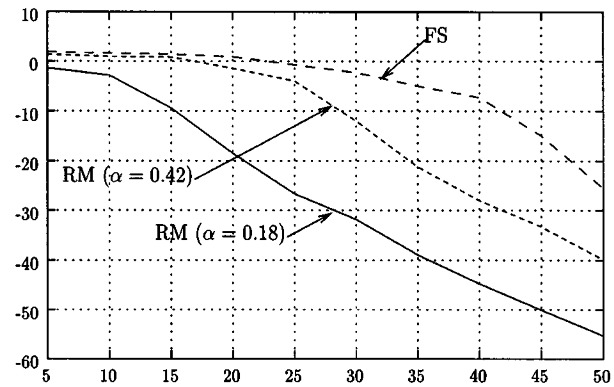

Fig. 6. Mean square error (in decibles) versus SNR.

As a conclusion, all these illustrations confirm the results of our heuristic approach.

C. *Simulation Results*

Once again, we consider Channel 1 ($\gamma = 0.2$). The experimental mean square error $\mathbb{E}\sum_{k=0}^{L}|\hat{h}_{T,k} - h_k|^2$ for FS and α-RM, $\alpha \in (0.18,\ 0.42)$ are represented in Fig. 6. The number of observations is $T = 300$. The number of Monte Carlo trials is 100. The SNR varies from 5–50 dB. Notice the (expected) improvement of performance in the case $\alpha = 0.18$ over the other cases (FS and $\alpha = 0.42$).

VI. Conclusion

In this paper, the α-repetition/modulation precoder is investigated on the blind second-order identification point of view. We have proved that the estimate of the unknown channel, relying on a structured subspace method, can show poor performance if the channel is bandlimited to $[-(\beta/2),\ (\beta/2)]$. More precisely, when $\alpha > (\beta/2)$, the estimate is likely to be the desired channel superimposed with undesired bandlimited spheroidal sequences. If the condition $\alpha \leq (\beta/2)$, no such bandlimited effect can be exhibited, and indeed, α-RM is then an appealing precoder in the sense that it allows a high-performance estimation of the unknown channel.

APPENDIX
JUSTIFICATION OF CLAIM 1

Recall that we address the problem of the conditioning of Q_α in the noiseless case, i.e., $S(e^{i2\pi f})$ is given by (8).

In the sequel, we call $\mathcal{I}_1 = [-(\beta/2), (\beta/2)]^c$ the complementary interval, in $[-(1/2), (1/2)]$, of $[-(\beta/2), (\beta/2)]$, so that

$$h(e^{2i\pi f}) \approx 0 \quad \text{if} \quad f \in \mathcal{I}_1.$$

Recall also that $\mathcal{I}_3 = \mathcal{I}_1 - \alpha$; we have

$$h\left(e^{2i\pi(f+\alpha)}\right) \approx 0 \quad \text{if} \quad f \in \mathcal{I}_3.$$

Let $\mathcal{I}_2 = (\mathcal{I}_1 \cup \mathcal{I}_3)^c$ and $\mathcal{I}_4 = \mathcal{I}_1 \cap \mathcal{I}_3$ In order to examine the numerical kernel of Q_α, we propose to show the consequences of the bandlimited character of $h(e^{i2\pi f})$ on the orthogonal projector Π. This projector is such that

$$\Pi \mathcal{R} \Pi^* = \mathbf{0}. \tag{9}$$

This equation simplifies accounting for the following relation:

$$\mathcal{R} = \int_{[-(1/2), (1/2)]} D_N(e^{i2\pi f}) D_N(e^{i2\pi f})^* \otimes S(e^{i2\pi f})\, df.$$

Indeed, (9) can be written as

$$\int_{[-(1/2), (1/2)]} \Pi(e^{i2\pi f}) S(e^{i2\pi f}) \Pi(e^{i2\pi f})^*\, df = \mathbf{0} \tag{10}$$

where $\Pi(e^{i2\pi f})$ is a $2(N+1) \times 2$ polynomial directly obtained from Π (see Section III). Rewriting $\Pi(e^{i2\pi f}) = (\Pi_1(e^{i2\pi f}), \Pi_2(e^{i2\pi f}))$ and accounting for (8), the subspace equation (10) gives, in particular [take the trace of (10)]

$$\int_{[-(1/2), (1/2)]} \left(\left|h(e^{i2\pi f})\right|^2 \Pi_1(e^{i2\pi f})^* \Pi_1(e^{i2\pi f}) + \left|h\left(e^{i2\pi(f+\alpha)}\right)\right|^2 \Pi_2(e^{i2\pi f})^* \Pi_2(e^{i2\pi f}) \right) df = 0.$$

In particular

$$\int_{\mathcal{I}_1} \left(\left|h(e^{i2\pi f})\right|^2 \Pi_1(e^{i2\pi f})^* \Pi_1(e^{i2\pi f}) + \left|h\left(e^{i2\pi(f+\alpha)}\right)\right|^2 \Pi_2(e^{i2\pi f})^* \Pi_2(e^{i2\pi f}) \right) df = 0.$$

On the other hand, $h(e^{i2\pi f}) \approx 0$ for $f \in \mathcal{I}_1$; hence

$$\int_{\mathcal{I}_1} \left|h\left(e^{i2\pi(f+\alpha)}\right)\right|^2 \Pi_2(e^{i2\pi f})^* \Pi_2(e^{i2\pi f})\, df \approx 0. \tag{11}$$

In general, notice that $h(e^{i2\pi(f+\alpha)})$ is nonzero in $\mathcal{I}_1$ except if $\mathcal{I}_4 = \mathcal{I}_1 \backslash \mathcal{I}_3$ is not an empty set, i.e., if $\alpha \geq 1 - \beta$ (see Figs. 7 and 8). Equation (11) then implies

$$\Pi_2(e^{i2\pi f})^* \Pi_2(e^{i2\pi f}) \approx 0 \quad \text{if} \quad f \in \mathcal{I}_1 \backslash \mathcal{I}_4.$$

A symmetrical analysis, this time considering the restriction of the integral (10) to the interval $\mathcal{I}_3$, shows that

$$\Pi_1(e^{i2\pi f})^* \Pi_1(e^{i2\pi f}) \approx 0 \quad \text{if} \quad f \in \mathcal{I}_3 \backslash \mathcal{I}_4.$$

We have proven the lemma.

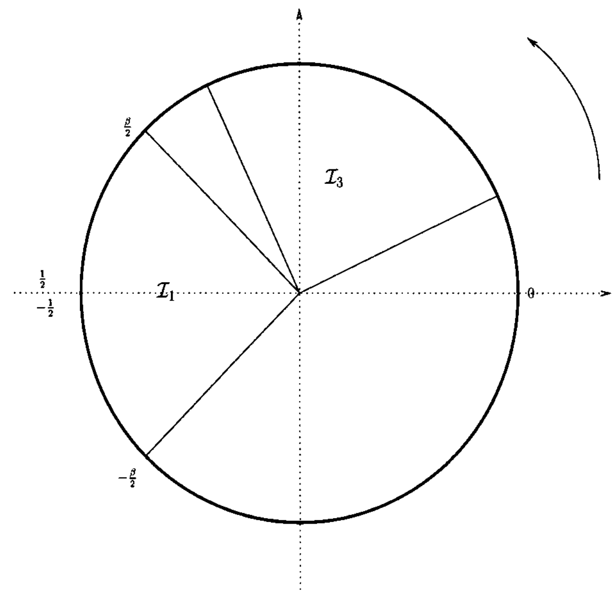

Fig. 7. Case 1: $\alpha \geq 1 - \beta$ and $\alpha \leq (\beta/2)$.

Lemma 1: As $h(e^{i2\pi f}) \approx 0$ for each $f \in \mathcal{I}_1$, the orthogonal projector Π is such that

$$\Pi_1(e^{i2\pi f})^* \Pi_1(e^{i2\pi f}) \approx 0 \quad \text{if} \quad f \in \mathcal{I}_3 \backslash \mathcal{I}_4 \tag{12}$$

$$\Pi_2(e^{i2\pi f})^* \Pi_2(e^{i2\pi f}) \approx 0 \quad \text{if} \quad f \in \mathcal{I}_1 \backslash \mathcal{I}_4. \tag{13}$$

We now examine the consequences of Lemma 1 on the numerical kernel of Q_α. For this, we introduce the set

$$\mathcal{W} = (\mathcal{I}_1 \cup \mathcal{I}_2 \cup (\mathcal{I}_2 + \alpha))^c.$$

We have the following result.

Lemma 2: If $\alpha \leq (\beta/2)$, we have $\mathcal{W} = \emptyset$. On the contrary, if $\alpha > (\beta/2)$, $\mathcal{W} = [(\beta/2) - \alpha,\ \alpha - (\beta/2)]$ The proof is simple. We provide, in Figs. 7–10, an illustration of the different configurations.

Suppose now that $\mathcal{W} \neq \emptyset$, which, according to Lemma 2, means that $\alpha > (\beta/2)$. Consider $\boldsymbol{k}_j$ as one of the smallest spheroidal wave sequence of the interval $\mathcal{W}^c$. There are

$$s = \text{int}((2\alpha - \beta)(L+1))$$

such sequences. We have, from Section IV-B

$$k_j(e^{i2\pi f}) \approx 0$$

if $f \in \mathcal{W}^c$ and $0 \leq j \leq s-1$. We aim at proving that $\boldsymbol{k}_j$ belongs to the numerical Kernel of Q_α; we therefore consider the quantity $\boldsymbol{k}_j^* Q_\alpha \boldsymbol{k}_j$, which, accounting for (5) and (6), can be expressed as

$$\boldsymbol{k}_j^* Q_\alpha \boldsymbol{k}_j = \int_{[-(1/2), (1/2)]} \left(k_j(e^{i2\pi f})^*\ k_j\left(e^{i2\pi(f+\alpha)}\right)^* \right) \cdot \Pi(e^{i2\pi f})^* \Pi(e^{i2\pi f}) \begin{pmatrix} k_j(e^{i2\pi f}) \\ k_j\left(e^{i2\pi(f+\alpha)}\right) \end{pmatrix} df. \tag{14}$$

The integral (14) may be cut into several ones.

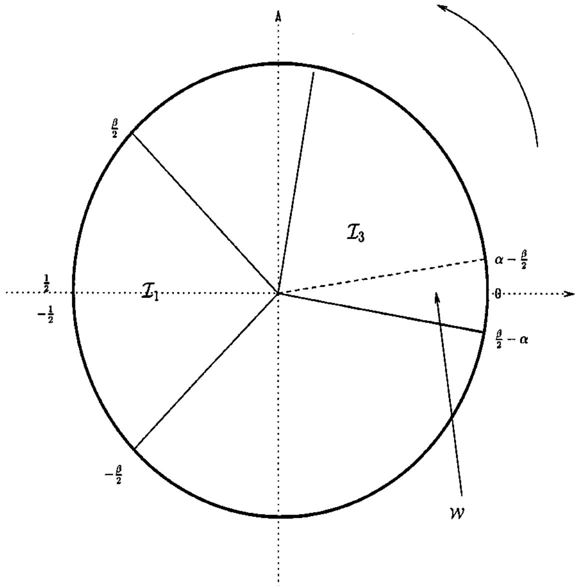

Fig. 8. Case 2: $\alpha \geq 1 - \beta$ and $\alpha > (\beta/2)$.

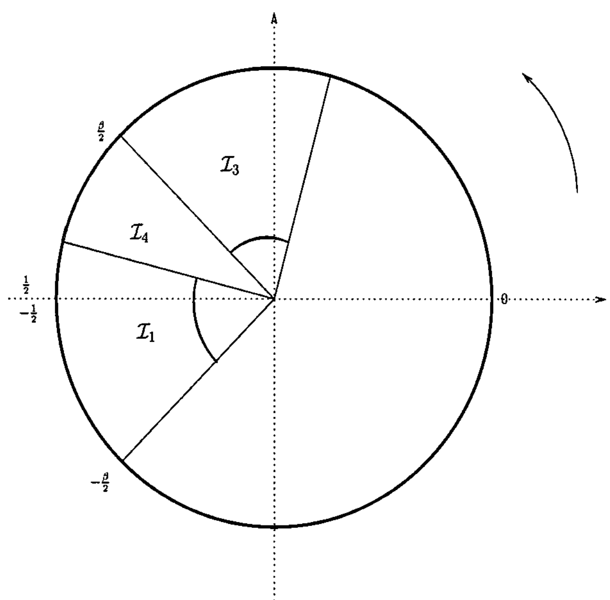

Fig. 9. Case 3: $\alpha \leq 1 - \beta$ and $\alpha \leq (\beta/2)$.

- Let us inspect $\int_{\mathcal{I}_1 \setminus \mathcal{I}_4}$. By Lemma 1, this integral equals

$$\int_{\mathcal{I}_1 \setminus \mathcal{I}_4} \left| k_j(e^{i2\pi f}) \right|^2 \Pi_1(e^{i2\pi f})^* \Pi_1(e^{i2\pi f})\, df.$$

  On the other hand, $k_j(e^{i2\pi f}) \approx 0$ on this interval $\mathcal{I}_1 \setminus \mathcal{I}_4$, and hence, the integral (14) is approximately null in the set $\mathcal{I}_1 \setminus \mathcal{I}_4$.
- Similarly, the integral on $\mathcal{I}_3 \setminus \mathcal{I}_4$ equals

$$\int_{\mathcal{I}_3 \setminus \mathcal{I}_4} \left| k_j\left(e^{i2\pi(f+\alpha)}\right) \right|^2 \Pi_2(e^{i2\pi f})^* \Pi_2(e^{i2\pi f})\, df$$

  and hence, as $k_j(e^{i2\pi(f+\alpha)}) \approx 0$ on this interval, the restriction of integral (14) on $\mathcal{I}_3 \setminus \mathcal{I}_4$ is also approximately null.

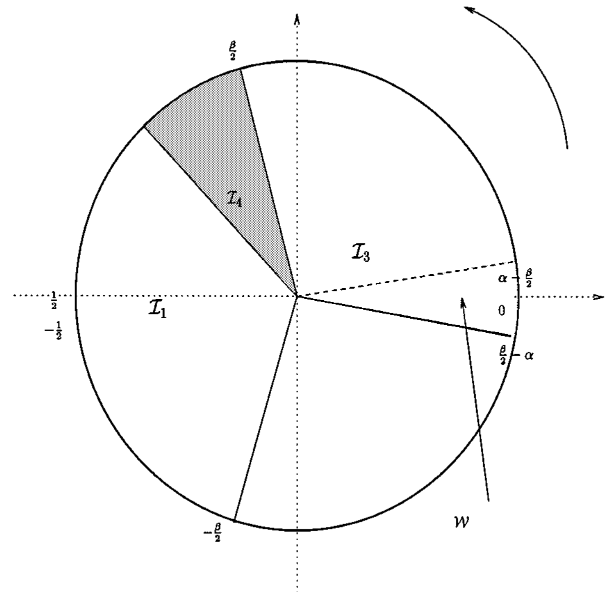

Fig. 10. Case 4: $\alpha \leq 1 - \beta$ and $\alpha > (\beta/2)$.

- On $\mathcal{I}_4 = \mathcal{I}_1 \cap \mathcal{I}_3$, both $k_j(e^{i2\pi f})$ and $k_j(e^{i2\pi(f+\alpha)})$ are approximately null, indicating that the integral (14) is numerically null on $\mathcal{I}_4$.
- Equation (14) remains to be inspected on $\mathcal{I}_2$. Notice that this term depends both on $k_j(e^{i2\pi f})$ and $k_j(e^{i2\pi(f+\alpha)})$ for $f \in \mathcal{I}_2$. As $k_j(e^{i2\pi f}) \approx 0$ for $f \in \mathcal{W}^c \supset \mathcal{I}_2 \cup (\mathcal{I}_2 + \alpha)$, it yields that both $k_j(e^{i2\pi f})$ and $k_j(e^{i2\pi(f+\alpha)})$ are approximately null on $\mathcal{I}_2$; hence, the component of integral (14) on $\mathcal{I}_2$ is numerically null.

This result is proven for any $(\boldsymbol{k}_j)_{j=0,\, s-1}$. One could consider

$$\boldsymbol{l} = \sum_{j=0}^{s-1} r_j \boldsymbol{k}_j + r_s \boldsymbol{h}. \tag{15}$$

It similarly yields

$$\boldsymbol{l}^* Q_\alpha \boldsymbol{l} \approx 0$$

thus showing that any vector $\boldsymbol{l}$, such that (15) holds, belongs to the numerical kernel of Q_α.

We have therefore exhibited a linear space spanned by the true channel $\boldsymbol{h}$ and some spheroidal wave functions on which the quadratic subspace matrix Q_α is almost null. This says that Q_α exhibits a so-called numerical kernel. Moreover, this numerical kernel is shown to be, *at least*, $s+1$dimensional. □

Remark 3: The matrix $\mathcal{R}$ may be ill conditioned for certain values of α owing to the bandlimited character of $h(e^{i2\pi f})$ (see [7]). In this case, $\mathcal{R}$ has a numerical kernel that is difficult to separate from the effective kernel. In other words, the matrix Π should be replaced by $\tilde{\Pi}$, which is the projection matrix onto the extended kernel. This implies to change Q_α in $\tilde{Q}_\alpha$. However, it is easy to prove that our analysis remains unchanged when replacing Q_α by $\tilde{Q}_\alpha$.

REFERENCES

[1] W. Gardner, "A new method of channel identification," *IEEE Trans. Signal Processing*, vol. 39, pp. 813–817, Aug. 1991.

[2] L. Tong, G. Xu, and T. Kailath, "A new approach to blind identification and equalization of multi-path channels," in *Proc. 25th Asilomar Conf.*, Pacific Grove, CA, 1991, pp. 856–860.

[3] G. B. Giannakis and S. Halford, "Blind fractionally spaced equalization of noisy FIR channels: Direct and adaptive solutions," *IEEE Trans. Signal Processing*, vol. 45, pp. 2277–2292, Sept. 1997.

[4] Y. Hua, "Fast maximum likelihood for blind identificltion of multiple FIR channels," *IEEE Trans. Signal Processing*, vol. 44, pp. 661–672, 1996.

[5] D. T. M. Slock, "Blind fractionally-spaced equalization, perfect-reconstruction filter-banks and multichannel linear prediction," *Proc. ICASSP*, vol. 4, pp. 585–588, 1994.

[6] G. Xu, H. Liu, L. Tong, and T. Iailath, "A deterministic approach to blind channel identification," *IEEE Signal Processing Lett.*, vol. 1, pp. 205–207, Dec. 1994.

[7] A. J. van der Veen, "Resolution limits of blind multi-user channels identification schemes: The baiid-limited case," *Proc. ICASSP*, pp. 2722–2725, 1996.

[8] Z. Ding, "Characteristics of band-limited channels unidentifiable from second-order statistics," *IEEE Signal Processing Lett.*, vol. 3, pp. 150–152, May 1996.

[9] E. Moulines, P. Duhamel, J.-F. Cardoso, and S. Mayrargue, "Subspace methods for the blind identification of multi-channel FIR filters," *IEEE Trans. Signal Processing*, vol. 43, pp. 516–525, Feb. 1995.

[10] P. Ciblat and P. Loubaton, "Second-order blind equalization: The band-limited case," in *Proc. ICASSP* Seattle, WA, May 1998, vol. 6, pp. 3401–3404.

[11] M. K. Tsatsanis and G. D. Giannakis, "Transmitter induced cyclostationarity for blind channel equalization," *IEEE Trans. Signal Processing*, vol. 45, pp. 1785–1794, July 1997.

[12] A. Chevreuil and P. Loubaton, "Modulation and second-order cyclo-stationarity: Structured subspace method and identifiability," *IEEE Signal Processing Lett.*, vol. 4, pp. 204–206, July 1997.

[13] E. Serpedin and G. B. Giannakis, "Blind channel identification and equalization with modulation-induced cyclostationarity," *IEEE Trans. Signal Processing*, vol. 46, pp. 1930–1944, July 1998.

[14] A. Chevreul, E. Serpedin, P. Loubaton, and G. Giannakis, "Blind channel identification and equalization using nonredundant periodic modulation precoders: Performance analysis," *IEEE Trans. Signal Processing*, to be published.

[15] G. B. Giatinakis, "Filterbanks for blind channel identification and equalization," *IEEE Signal Processing Lett.*, vol. 4, pp. 184–187, May 1997.

[16] A. Scaglione, S. Barbarossa, and G. Giannakis, "Redundant filterbank precoders and equlizers—Part I: Unification and optimal design—Part II: Blind channel estimation, synchronization, and direct equalization," *IEEE Trans. Signal Processing*, vol. 47, pp. 1988–2022, 1999.

[17] A. Chevreuil and P. Loubaton, "Repetition/modulation of the symbols: Blind equalization versus capacity," *Proc. SPIE*, vol. 3461, pp. 47–54, July 1998.

[18] K. Abed-Meraim, J. F. Cardoso, A. Gorokhov, P. Loubaton, and E. Moulines, "On subspace methods for blind identification of single-input/milti-output FIR systems," *IEEE Trans. Signal Processing*, vol. 45, pp. 42–56, Jan. 1997.

[19] D. Slepian, "Prolate spheroidal wave functions. Fourier analysis and uncertainty," *Bell Syst. Tech. J.*, vol. 57, no. 5, May–June 1978.

[20] D. Thomson, "Spectrum estimation and harmonic analysis," *Proc. IEEE*, vol. 70, pp. 1055–1096, Sept. 1982.

[21] K. Buckley, "Spatial/spectral filtering with linearly constrained minimum variance beamformers," *IEEE. Trans. Acoust. Speech, Signal Processing*, vol. ASSP-35, pp. 249–266, 1985.

[22] P. Forster and G. Nezzozi, "Application of spheroidal sequences to array processing," in *Proc. ICASSP*, Apr. 1987, pp. 2267–2271.

[23] A. Clievreuil, F. Desbouvries, A. Gorokliov, P. Loubaton, and C. Vignat, "Blind equalization in the presence of jammers and unknown noise. Solutions based on second-order cyclostationtry statistics," *IEEE Trans. Signal Processing*, vol. 46, pp. 259–263, Jan. 1998.

[24] L. Deneire and D. T. M. Slock, "Blind channel identification based on cyrclic statistics," *Proc. Inst. Elect. Eng., Radar, Sonar Navig., Special Issue in Antenna Array Processing Techniques*, vol. 145, no. 1, Feb. 1998.

[25] C. Becclietti, G. Jacovitti, and G. Scarano, "Fast blind identification of FIR communications channels," in *Proc. ICASSP*, Seattle, WA, 1998, pp. 3405–3409.

[26] A. Chevreuil, E. Serpedin, P. Loubaton, and G. Giannakis, "Blind channel identification and equalization using nonredundant periodic modulation precoders: Performance analysis," *Proc. ICASSP*, vol. 6, pp. 3397–3401.

Philippe Ciblat was born in Paris, France, in 1973. He received the B.Sc. degree in mathematics from University of Paris in 1994. He also received the Engineer degree from Ecole Nationale Supérieure des Télécommunications, Paris, and the M.Sc. degree in signal processing from Orsay University, Orsay, France, in 1996. He is currently pursuing the Ph.D. degree at the University of Marne-la-Vallée, Champs sur Marne, France. His research areas include statistical and digital signal processing, especially blind equalization, frequency estimation, and asymptotic performance analysis.

Antoine Chevreuil was born in Caen, France, in 1971. He received the M.Sc. and Ph.D. degrees from the Ecole Nationale des Télécommunications, Paris, in 1994 and 1997, respectively.

In 1998, he held a post-doctoral position with the Department of Telecommunications, University of Louvain-la-Neuve, Belgium. He has been an Assistant Professor with the University of Marne-la-Vallée, Champs sur Marne, France, since 1999. His present topics of interest are blind equalization, cyclostationary processes for communications, and source separation.

Philippe Loubaton (M'88) was born in 1958 in Villers Semeuse, France. He received the M.Sc. and Ph.D. degrees from Ecole Nationale Supérieure des Télécommunications (ENST), Paris, France, in 1981 and 1988, respectively.

From 1982 to 1986, he was Member of Technical Staff, Thomson-CSF/RGS, where he worked in digital communications. From 1986 to 1988, he was with the Institut National des Télécommunications as an Assistant Professor of Electrical Engineering. In 1988, he joined ENST, where he worked in the Signal Processing Department. Since 1995, he has been Professor of Electrical Engineering at the University of Marne la Vallée, Champs sur Marne, France. His present research interests are in statistical signal processing and digital communications with a special emphasis on blind equalization, multiuser communication systems, and multicarrier modulations.

Dr. Loubaton is currently Associate Editor for the IEEE TRANSACTIONS ON SIGNAL PROCESSING and is a Member of the IEEE Signal Processing for Communications Technical Committee.